Thermal Denaturation: A Method to Rank Slow Binding, High-Affinity P38α MAP Kinase Inhibitors

Rachel R. Kroe,*,† John Regan,‡ Al Proto,# Gregory W. Peet,† Tapon Roy,§ Laura D. Landro,⊥ Natalie G. Fuschetto,† Christopher A. Pargellis,† and Richard H. Ingraham†

Department of Immunology and Inflammation, Boehringer Ingelheim Pharmaceuticals, Inc., 900 Ridgebury Road, P. O. Box 368, Ridgefield, Connecticut 06877, and Department of Medicinal Chemistry, Boehringer Ingelheim Pharmaceuticals, Inc. 900 Ridgebury Road, P. O. Box 368, Ridgefield, Connecticut 06877, Universidad Autonoma de Guadalajara, Guadalajara, Jalisco 45110, Mexico, Department of Biometrics and Data Management, Boehringer Ingelheim Pharmaceuticals, Inc. 900 Ridgebury Road, P. O. Box 368, Ridgefield, Connecticut 06877, and Bristol Central High School, 480 Wolcott Street, Bristol, Connecticut 06010

Received March 13, 2003

It has been reported that the diaryl urea class of p38α inhibitors binds to p38 map kinase with both high affinity and slow binding kinetics (Pargellis et al. *Nat. Struct. Biol.* **2002**, *9*, 268−272). The slow binding kinetics of this class of inhibitors is believed to be the result of binding to an allosteric pocket adjacent to the p38α active site. The use of traditional kinetic and equilibrium methods to measure the binding affinity of this class of compounds has created many challenges for determination of structure-activity relationships (SAR). The thermal denaturation method provides a means of measuring high-affinity interactions. In this paper, the method of thermal denaturation will be described as it has been applied to the diaryl urea class of p38 map kinase inhibitors.

Introduction

The mitogen-activated protein kinase (MAPK) signal transduction pathways are activated in response to inflammatory mediators released during acute and chronic disease. There are three major MAPK pathways, extracellular-regulated protein kinase (ERK), cJUN NH2-terminal kinase (JNK) and p38 mitogen-activated kinase (p38 MAPK). Each pathway has multiple isoforms that may play different roles and be differentially expressed in various tissues. Activation of the p38 MAPK pathway results in the recruitment of leukocytes and the activation of immune and inflammatory cells. Acute and chronic inflammation is thought to be central to the pathogenesis of many diseases such as rheumatoid arthritis, asthma, chronic obstructive pulmonary disease, Crohn's disease, and psoriasis. Inhibitors aimed at reducing the production of inflammatory mediators are now being developed with the hope of providing an effective treatment for inflammatory diseases.

In our search for inhibitors against the alpha isoform of p38 MAPK, a class of inhibitors has been identified that binds to p38α MAPK with high affinity and slow binding kinetics.[1] These compounds bind to p38α by a novel mechanism that utilizes not only the ATP binding site and the kinase specificity pocket but also an allosteric pocket, formation of which requires a large conformational change in the protein. The slow binding kinetics seen with the diaryl urea class of p38 MAPK inhibitors is consistent with the requirement for structural rearrangement of the protein. The unique binding mode of the diaryl urea class of p38 MAPK inhibitors has made it difficult to accurately measure the binding affinity of these compounds using traditional equilibrium methods.

Various researchers have measured changes in protein thermal stability as a function of ligand concentration to determine binding affinity.[2−6] The method described in this paper follows an earlier method described by Brandts and Lin on the use of differential scanning calorimetry (DSC) to study protein interactions.[2] It has been shown that one of the major advantages of the thermal denaturation method is the ability to measure large binding constants. A second potential advantage of this technique, not previously stated, is in the measurement of association constants for interactions that have slow binding kinetics. To accurately measure association constants for ligands with slow kinetics using equilibrium methods requires very long incubation times over which the protein may or may not be stable. Since the thermal denaturation method does not directly monitor the binding interaction, experiments can be performed at concentrations of ligand well above the binding constant where binding kinetics are not limiting. As a result, experiments can be run more rapidly and with a higher degree of accuracy. For the case of the diaryl urea class of p38α inhibitors that bind with both high affinity and slow kinetics, the thermal denaturation method is the preferred method for the measurement of binding affinity to provide the throughput required for SAR.

Theory

There are two equilibria occurring during the thermal denaturation experiment (eq 1). The first equilibrium

* To whom correspondence should be addressed. Phone: (203) 778−7740. Fax: (203) 791−6196. E-mail: rkroe@rdg.boehringer-ingelheim.com.

† Department of Immunology and Inflammation, Boehringer Ingelheim Pharmaceuticals, Inc.

‡ Department of Medicinal Chemistry, Boehringer Ingelheim Pharmaceuticals, Inc.

Universidad Autonoma de Guadalajara.

§ Department of Biometrics and Data Management, Boehringer Ingelheim Pharmaceuticals, Inc.

⊥ Bristol Central High School.

10.1021/jm030120s CCC: $25.00 © 2003 American Chemical Society
Published on Web 09/20/2003

constant, K_a, describes the small molecule inhibitor binding to p38α. The second equilibrium constant, K_{unfold}, describes the transition of p38α from a folded to an unfolded state.

$$\text{p38}\alpha + \text{L} \xrightarrow{K_a} \text{p38}\alpha\text{L} \quad K_a = \frac{[\text{p38}\alpha\text{L}]}{[\text{p38}\alpha][\text{L}]}$$

$$\text{p38}\alpha_{fold} \xrightarrow{K_{unfold}} \text{p38}\alpha_{unfold} \quad K_{unfold} = \frac{[\text{p38}\alpha_{unfold}]}{[\text{p38}\alpha_{fold}]} \quad (1)$$

Following the derivation of Brandts and Lin, these two equilibrium constants can be combined to yield an expression for the equilibrium binding constant at the melting temperature as a function of the free energy of unfolding and the total ligand concentration (eq 2)

$$K_{a,Tm} = \frac{\left(\exp \frac{-\Delta G_{unfold,Tm,L}}{RT_m}\right) - 1}{[\text{L}]} \quad (2)$$

where K_a is the equilibrium binding constant for the small molecule inhibitor at the melting temperature, $\Delta G_{unfold,Tm,L}$ is the free energy of unfolding for p38α in the presence of ligand, L is the free ligand concentration, R is the gas constant and T_m is the melting temperature. This derivation assumes that (1) the unfolding transition is two-state; (2) ligand will bind only to the folded form; (3) all ΔC_p values are temperature independent; (4) all reactions are reversible; (5) all measurements are made at equilibrium; and (6) all activity coefficients are unity.[2] Rewriting $\Delta G_{unfold,Tm,L}$ in terms of enthalpy and entropy results in eq 3

$$K_{a,Tm} = \frac{\exp - \left(\frac{\Delta H_{T0}}{R}\left(\frac{1}{T_m} - \frac{1}{T_0}\right) + \frac{\Delta C_p}{R}\left(1 - \frac{T_0}{T_m} - \ln\frac{T_m}{T_0}\right)\right) - 1}{[\text{L}]} \quad (3)$$

where $K_{a,Tm}$ is the equilibrium binding constant for the small molecule inhibitor, ΔH_{T0} is the enthalpy of unfolding for the unliganded p38α, T_0 is the melting temperature for the unliganded p38α, T_m is the melting temperature for the p38α inhibitor complex, ΔC_p is the change in heat capacity for unfolding of the unliganded p38α, and L is the free ligand concentration. Each of the terms in this equation can be measured allowing for the calculation of K_a for the inhibitor binding at the melting temperature.

To compare the binding constants of different small molecule inhibitors for an enzyme, the binding constant calculated at the melting temperature must be converted to a reference temperature. This is achieved by using the following equation.

$$K_a = K_{a,Tm} \exp\left(-\frac{\Delta H_L}{R}\left(\frac{1}{T_r} - \frac{1}{T_m}\right) + \frac{\Delta C_{pL}}{R}\left(\ln\frac{T_r}{T_m} + 1 - \frac{T_r}{T_m}\right)\right) \quad (4)$$

where $K_{a,Tm}$ is the binding constant calculated at the melting temperature, ΔH_L is the enthalpy of ligand binding at the melting temperature, ΔC_{pL} is the change in heat capacity for the small molecule binding to p38α, T_r is the reference temperature, and T_m is the melting temperature for the liganded p38α.

Experimental Section

A. Materials. Compounds were synthesized as described in Regan et al.[7]

Cloning, Expression, and Purification of Murine p38α MAPK. The full-length open reading frame of murine p38α MAPK was originally obtained by RT-PCR amplification of murine macrophage RNA and matches accession gi:15126598 in genbank. The p38α gene was initially ligated into pGEMT (Promega) and subsequently subcloned into pET15b adding a noncleavable 5His affinity tag for purification (Novagen). The resulting expression vector was transformed into $CaCl_2$-competent B834(DE3) pLysS cells by heat shock. The expression host was grown in LB media containing 100 μg/mL carbenicillin and 34 μg/mL chloramphenicol. For scale-up expression, a 1 L culture was grown overnight to saturation and was used to inoculate a 15 L working volume fermenter (MBR BioRactor, Switzerland). The fermentation culture was grown to an OD_{600} of 1.0 at 37 °C with saturating oxygen. The culture was then induced with 0.1 mM IPTG for 2.5 h under the same conditions. Cells were harvested by centrifugation and stored at −80 °C until purification.

Soluble murine p38α was extracted from cell pellets and resuspended in 20 mM Tris-HCl, pH 8.0, 300 mM NaCl, 10% glycerol, and EDTA-free protease inhibitor tablets (Roche) (buffer A). The suspended pellet was sonicated for three 5-min cycles using a Branson 450 Sonifier at a 50% duty cycle and level 5 output allowing for 10 min cooling on ice between cycles. After sonication of the sample, the lysate was centrifuged at 44 000 rpm for 1 h using a Beckman LE80 centrifuge with a Ti45 rotor. The clarified soluble lysate was loaded onto a Ni−NTA Superflow column (Qiagen) equilibrated with buffer A. The column was then washed with buffer A, followed by buffer A with 10 mM imidazole. The column was eluted with 20 mM Tris-HCl, pH 8.0, 250 mM imidazole, 300 mM NaCl, and 10% glycerol. Chromatography was monitored at 280 nm and 2 mM dithiothreitol and 1 mM EDTA were added to collected fractions. Pooled fractions were dialyzed into 20 mM Tris-HCl, pH 7.5, 75 mM NaCl, 5% glycerol, and 2 mM dithiothreitol. Ion-exchange chromatography of the pooled fractions was performed using a 25Q column (Biorad, Hercules, CA) equilibrated in 20 mM Tris-HCl, pH 7.5, 50 mM NaCl, 5% glycerol, and 2 mM DTT. A 50 mM to 1 M NaCl gradient was used for elution. Fractions were pooled, concentrated, and then loaded onto a Sephacryl High-Resolution S100 26/60 column (Amersham) equilibrated in 20 mM Tris-HCl, pH 7.5, 150 mM NaCl, 5% glycerol, and 2 mM DTT. Column fractions were concentrated, analyzed by SDS−PAGE, and pooled based on purity. The final p38α concentration was determined by a spectrophotometer using a molar extinction coefficient at 280 nm of 49 850 M^{-1} cm^{-1}.

Human p38α MAPK was expressed and purified as previously published.[8]

B. Methods. Differential Scanning Calorimetry. The DSC experiments were performed using a Microcal VP-DSC from Microcal, Inc. (Northampton, MA). The sample cell of the calorimeter was loaded with 1−2 mg/mL of murine p38α MAPK in a pH 7.0 buffer containing either low salt (10 mM sodium phosphate, 1 mM Tris(2-carboxyethyl)phosphine hydrochloride (TCEP)) or moderate salt (10 mM sodium phosphate, 100 mM NaCl, 1 mM TCEP). For experiments where inhibitor is present, inhibitors were added at twice the protein concentration resulting in a final dimethyl sulfoxide (DMSO) concentration of 0.5%. The reference cell was filled with the corresponding dialysate buffer with added DMSO when appropriate. All solutions were degassed for 8 min and then scanned from 20 to 90 °C at a rate of either 1 or 0.2 °C/min. Baseline scans,collected with dialysate buffer in both the sample and reference cells, were subtracted from the protein scans and the corrected data were adjusted according to the protein concentration. Data were analyzed using Origin DSC data analysis software (version 5.0).

Isothermal Titration Calorimetry. The isothermal titration calorimetry (ITC) experiments were performed using a Microcal VP−ITC from Microcal, Inc. (Northampton, MA). The sample cell of the calorimeter was loaded with concentrations of test compound ranging from 10 to 30 μM in a pH 7.0 buffer containing 10 mM sodium phosphate, 1 mM TCEP, and

1% DMSO. The syringe was loaded with concentrations of murine p38α MAPK ranging from 75 to 225 μM in the same buffer. All solutions were degassed for 8 min. Titrations were performed at 25 °C with injection volumes ranging from 8 to 15 μL and a spacing of 500 s. After completion of the titration, baselines were manually drawn and subtracted from the data. The data were zeroed assuming that the final injections of each titration represent only the heat of dilution. Data were fit using a one-site binding model available in the Origin ITC data analysis software (version 5.0).

UV−Thermal Melt. The UV-thermal melt experiments were carried out using a Perkin-Elmer Lambda 40 spectrophotometer equipped with a PTP-6 Peltier system and six-cell linear transporter. For each measurement, a quartz cuvette was loaded with 2.5 μM murine p38α MAPK and 25 μM inhibitor in a pH 7.0 buffer containing 10 mM sodium phosphate, 100 mM NaCl, and 1 mM TCEP. Absorbance data at 230 nm were collected as the temperature was scanned from 25 to 80 °C at a ramp rate of 0.2 °C/min. The melting temperature for each sample was calculated as the maximum deflection point of the first derivative of the melting transition using the Perkin-Elmer Templab software (version 1.62). The circular dichroism thermal melt was performed on a Jasco J720 equipped with a PTC-343 Peltier device.

Fluorescence Exchange Curve Assay. The fluorescence exchange curve experiments were carried out as described previously.[1] These studies were performed in a pH 7.0 buffer containing 20 mM bis-tris propane, 2 mM EDTA, 0.01% NaN_3, and 0.15% *n*-octylglucoside. The exchange curve assays were run as two half-reactions using an SLM Aminco Bowman Series 2 model SQ-340 fluorescence detector. In the first half reaction, p38α MAPK and SK&F 86002 are preincubated for 3 min. In the second half reaction, p38α MAPK is preincubated with inhibitor for 60 min. A net dissociation of the fluoroprobe is observed for the first half-reaction, and a net association is observed for the second half-reaction. The raw data from both half-reactions are fit simultaneously to an equation describing simple competitive inhibition.

Data from the fluorescence exchange curve assay were collected using either murine or human p38α MAPK. The on and off rate kinetics and the equilibrium binding affinities for a series of compounds binding to either murine or human protein were compared and found to be identical (data not shown). This result is not surprising since the amino acid sequence for murine and human p38α MAPK varies by only two residues (L47/H47 and T262/A262) both of which are located on the surface of p38α MAPK.

Propagation of Errors. The $K_{a,Tm}$ and K_a binding constants obtained from eqs 3 and 4 have standard errors that are obtained by propagating the errors in their components which have variability from replicate measurements. In general, for any function $y = f(x_1, x_2, x_3, ..., x_n)$, where $x_1, x_2, x_3, ..., x_n$ are components with associated errors, the propagated error on y is obtained by quadrature as follows:

$$\text{Error } (y) = \sqrt{\sum_{i=1}^{n} (\partial y/\partial x_i)^2 s_{x_i}{}^2}$$

where s_{xi} is the error associated with x_i.[9−10]

This procedure is first applied to eq 3 to obtain the propagated error on $K_{a,Tm}$ and then is used on eq 4 to obtain the propagated error on K_a. This technique is also applied to the regression line displayed in Figure 4. For these data, since both axes have associated measurement error, inverse regression (regression on exchanged axes) is a valid procedure.[11,12] The statistical errors on log K_a obtained from the inverse regression fit are then propagated as described above via the antilog function to obtain the statistical errors on K_a. Computations were made using SAS statistical software version 8.2 (SAS Institute, Cary, NC) and Mathematica software version 4.2 (Wolfram Research, Champaign, IL).

Results

Measurement of the Change in Heat Capacity and Enthalpy of Unfolding for p38α. A DSC scan of unliganded p38α under low salt conditions is shown in Figure 1A. The unfolding of p38α is irreversible under low salt conditions. This was determined by comparing the ΔH_{T0} measured after a full scan to the value measured after partially scanning to 40 °C then rescanning from 25 to 80 °C. The enthalpy measured after the partial scan was 50% of the value measured by a single full scan. The unfolding of p38α is also irreversible under moderate salt conditions. The low salt conditions enabled measurement of ΔC_p since the protein did not precipitate at temperatures beyond the melting temperature as seen under the moderate salt conditions. The enthalpy of unfolding for the unliganded p38α (ΔH_{T0}) was determined by integrating the area under the DSC curve. The measured value of 108 ± 14 kcal/mol was calculated by averaging the results from five experiments. The change in heat capacity for unliganded p38α (ΔC_p) is represented by the change in baseline before and after the melting transition. The measured value of 2.5 ± 0.9 kcal/mol K was fit from the data and calculated as the average of five experiments.

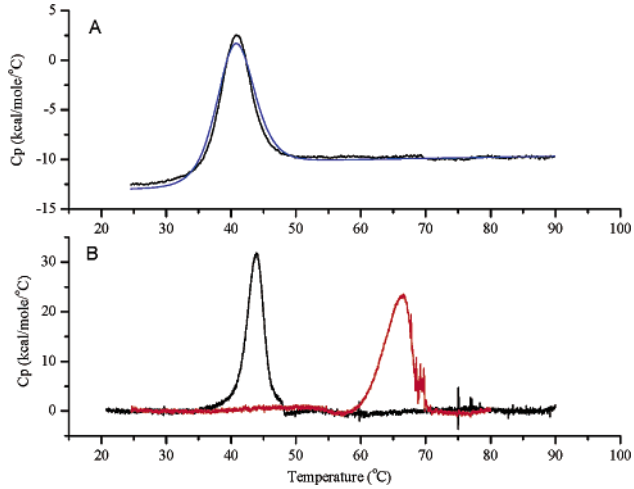

Figure 1. DSC curve for murine p38α in the presence and absence of compound 10. (A) DSC curve for unliganded murine p38α (black) and fit of data (blue) in low salt buffer. (B) DSC curve for unliganded murine p38α (black) and murine p38α with 2-fold excess compound 10 (red) in moderate salt buffer.

DSC scans of p38α in the presence and absence of inhibitor (compound 10, previously published as BIRB 796)[13] are shown in Figure 1B. These experiments were conducted in the moderate salt buffer. These data show the shift in T_m that occurs in the presence of 2-fold excess inhibitor. In addition, it can be seen that the T_m for the unliganded p38α in the low salt buffer shifts from 40.6 ± 0.4 to 45.2 ± 1.6 °C when measured in the moderate salt buffer.

UV−Thermal Melts. Ideally, DSC scans would be used to measure the melting temperature for p38α in the presence of inhibitor. However, due to limited throughput and the requirement for large amounts of protein, melting temperatures were determined by UV−thermal melting experiments. Initially, the thermal transition was observed by circular dichroism. A loss of secondary structure was seen as p38α converted from a folded to an unfolded state (data not shown). This transition could be detected by monitoring either the CD or absorbance signal at 230 nm. To further increase

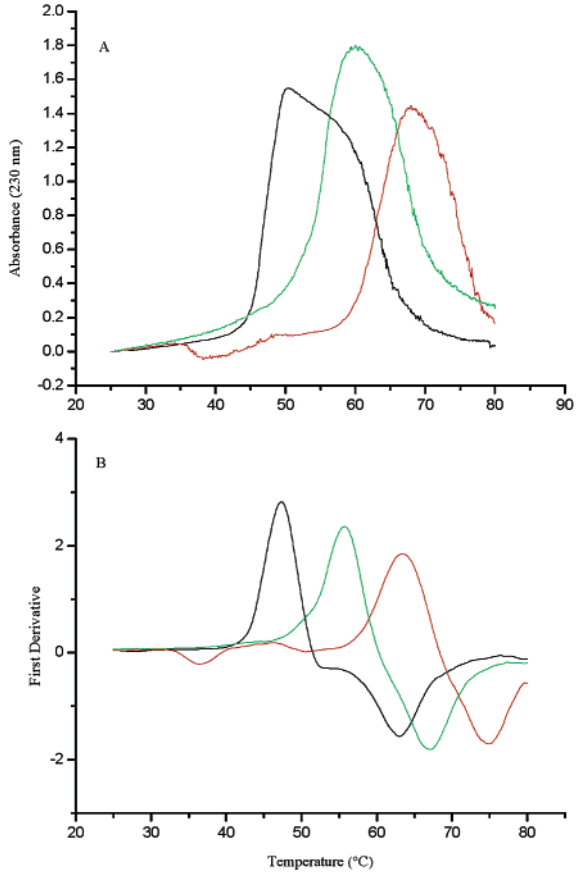

Figure 2. UV Thermal melt of murine p38α with inhibitors. (A) UV-thermal melt of murine p38α (black), murine p38α + 10-fold excess compound 6 (green), and murine p38α plus 10-fold excess compound 10 (red) in moderate salt buffer. (B) First derivative of the UV−thermal melt raw data for murine p38α (black), murine p38α + 10-fold excess compound 6 (green), and murine p38α plus 10-fold excess compound 10 (red) in moderate salt buffer.

throughput, the melting transition was observed using a UV−Vis spectrophotometer outfitted with a six-cell linear transporter and a Peltier accessory. Examples of UV-thermal melt data for two compounds performed in the spectrophotometer are shown in Figure 2A. The decrease in UV signal that occurs after the melting transition is the result of protein precipitation. The melting temperature is calculated as the maximum deflection point of the first derivative (Figure 2B).

All of the melting temperatures for p38α in the presence of inhibitors were measured under moderate salt conditions. The melting temperature for unliganded p38α as determined by UV−thermal melt under the moderate salt conditions is in good agreement with the melting temperature as determined by DSC, 46.5 ± 0.6 versus 45.2 ± 1.6 °C, respectively. Since all of the melting temperatures for the p38α were measured under moderate salt conditions the ΔH_{T0} had to be corrected to account for the shift in T_m between the two buffer conditions. This was done using the following equation

$$\Delta H = \Delta H_r + \Delta C_p(T - T_r) \quad (5)$$

where ΔH_r is the enthalpy of unfolding determined in the low salt buffer, T_r is the melting temperature

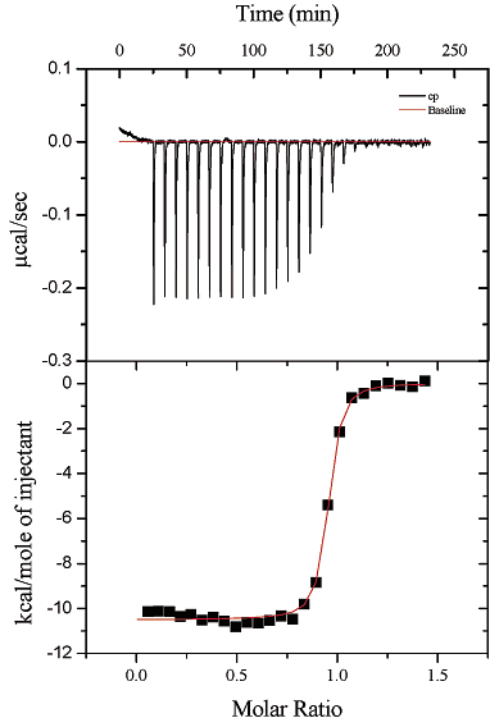

Figure 3. Calorimetric titration of murine p38α into sample cell containing compound 4 at 25 °C in 10 mM sodium phosphate, pH 7.0 and 1 mM TCEP. Fit parameters: $N = 0.93$, $K_a = 1.036 \times 10^8 \pm 1.638 \times 10^7$, $\Delta H = -10.5 \pm 0.06$ kcal/mol, and $\Delta S = 1.46$ cal/mol K.

measured in the low salt buffer, and T is the melting temperature measured in the moderate salt buffer. The corrected value for ΔH_{T0} is 123 kcal/mol. At this point, the $K_{a,Tm}$ for each inhibitor can be calculated using eq 3 (Table 1). For these calculations, the free ligand concentration [L] was assumed to be the total ligand concentration minus the protein concentration.

Isothermal Titration Calorimetry. Conversion of $K_{a,Tm}$ to a reference temperature is achieved using eq 4. The two parameters necessary for this calculation are the enthalpy of ligand binding (ΔH_L) at the melting temperature and the change in heat capacity for ligand binding (ΔC_{pL}). ITC was used to measure ΔH_L for 10 inhibitors with affinities for p38α ranging from K_d = 2.4 μM to 46 pM. A representative ITC data set showing data for compound 4 is shown in Figure 3. While ITC cannot be used to determine association constants for binding interactions as strong as 46 pM it can be used to very accurately measure ΔH_L. The change in heat capacity for ligand binding was measured for compound 4 and found to be −85 cal/mol K (data not shown). This value was assumed to be representative of all of the compounds within this structural class and used generically. The enthalpy of ligand binding for each compound measured at 25 °C was corrected to the appropriate melting temperature by eq 5 using the generic ΔC_{pL}. Using the corrected values of ΔH_L and the ΔC_{pL} for compound 4, the $K_{a,Tref}$ (25 °C) was calculated for each of the 10 inhibitors using eq 4 (Table 1). Since ΔH_L is a small number, the conversion to T_R will not dramatically change K_a, as can be seen in Table 1. The conversion becomes more critical as the value of ΔH_L increases.

To alleviate the need for measuring ΔH_L for each inhibitor assayed, the T_m for each of the 10 inhibitors

Table 1

Cmpd. No.	Structure	ΔH^a (kcal/mol)	$T_m{}^b$ (°C)	$K_{d,T_m}{}^c$ (nM)	$K_{d,Tref}{}^d$ (nM)	$K_d{}^e$ (nM)	$K_d{}^f$ (nM)
1	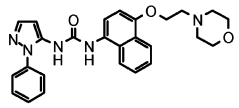	-4.3 ± 1.3	49.1 ± 0.4	6070 ± 1520	2400 ± 644		1181
2	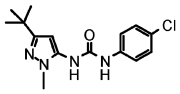	-5.6 ±0.04	49.2 ± 0.1	5850 ± 668	1950 ± 223	1160	1152
3	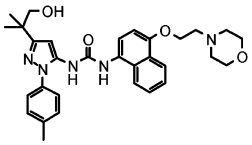	-11.4 ± 0.2	53.0 ± 1.6	493 ± 339	56.4 ± 39.2	36	20
4	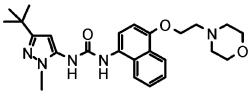	-10.1 ± 0.5	54.5 ± 2.8	210 ± 245	25.7 ± 30.2	23	10
5	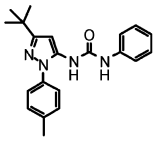	-11.6 ± 0.7	54.8 ± 0.5	177 ± 58.8	16.8 ± 5.8	21	5
6	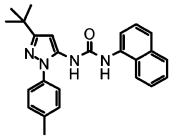	-11.6 ± 0.2	55.5 ± 0.4	118 ± 37.6	10.6 ± 3.4	1	
7	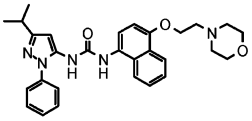	-14.1 ± 0.5	56.6 ± 0.2	62.8 ± 20.7	3.4 ± 1.1	6*	
8	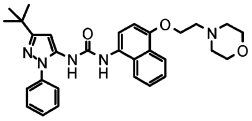	-12.7 ± 0.1	61.0 ± 0.2	5.3 ± 2.4	0.231 ± 0.11	0.09	
9	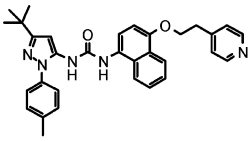	-12.0 ± 0.4	62.4 ± 0.3	2.4 ± 1.2	0.104 ± 0.053	0.5	
10	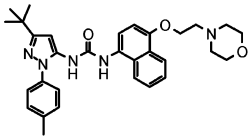	-12.6 ± 0.3	63.5 ± 0.4	1.3 ± 0.71	0.046 ± 0.025	0.1	

[a] Enthalpy of ligand binding as measured by ITC. [b] Melting temperature measured by UV−thermal melt. [c] Dissociation constant at T_m expressed as $1/K_a$. [d] Dissociation constant at T_{ref} expressed as $1/K_a$. [e] Dissociation constant measured using the fluorescence exchange curve assay expressed as $1/K_a$. [f] Dissociation constant fit from ITC data. *Data generated using murine p38α. All other data in this table were generated with human p38α. The error on ΔH and T_m is calculated as the standard deviation. The error on all other values is calculated as the standard error.

was plotted versus log $K_{a,Tref}$ (Figure 4). A linear fit of this graph results in an equation that can be used to estimate $K_{a,Tref}$ from any T_m value. The average error for a K_a value calculated using this equation is ±16.1% (sd = 4.2%). It remains to be seen whether similar plots of T_m versus log $K_{a,Tref}$ derived for other enzyme targets and drug scaffolds result in this same linear relationship.

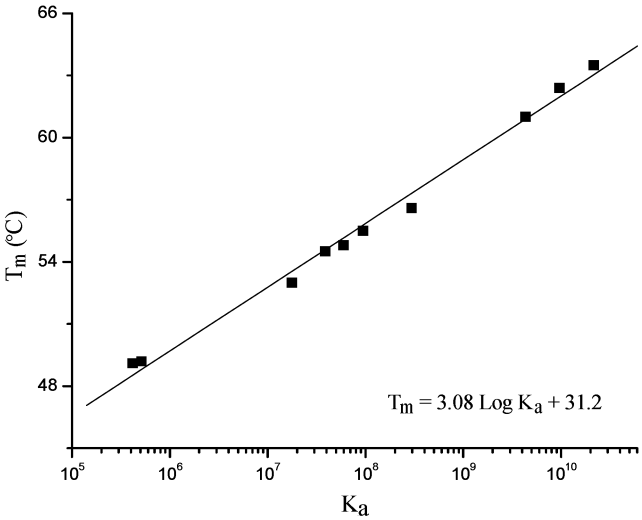

Figure 4. A semilog plot of T_m versus $K_{a,Tref}$ for compounds 1−10.

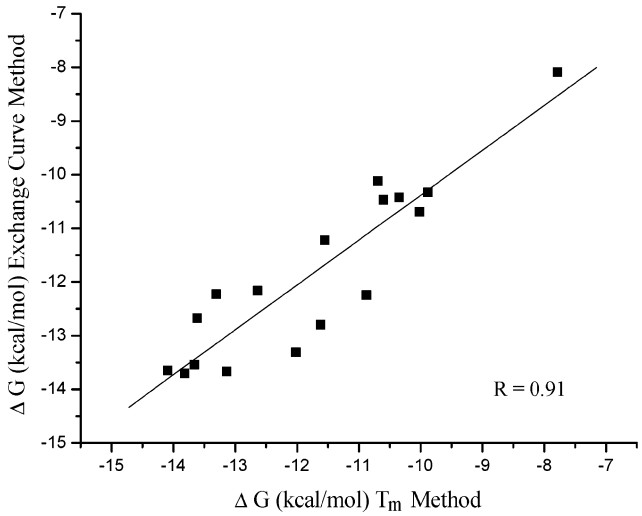

Figure 5. Correlation graph comparing the Gibbs free energy of binding calculated for various inhibitors using the fluorescence exchange curve method versus the thermal denaturation method.

Comparison of Thermal Denaturation method to Fluorescence Exchange Curve method. A fluorescence exchange curve assay was used to measure k_{on} and k_{off} for several p38α inhibitors. The dissociation constant for each of these compounds was calculated as the ratio of k_{off}/k_{on}. These values were then compared to those estimated using the thermal denaturation method. A plot of $\Delta G_{Tm\ method}$ versus $\Delta G_{exchange\ curve\ method}$ is shown in Figure 5. Linear regression of this line gives a correlation coefficient of 0.91. The correlation between these two methods is remarkably good considering the indirect nature of the thermal denaturation method and the complications of working with small molecule inhibitors that do not have ideal physicochemical properties. The reasonable correlation also supports treating the unfolding reaction as reversible even though it was shown to be irreversible under both low and moderate salt conditions as well as in the presence of inhibitors.

Discussion

Kinases are attractive target biomolecules for the treatment of numerous autoimmune and inflammatory diseases as well as cancer. Currently, crystallographic structures are available for many kinase targets and are currently being pursued for many more.[14] In general, the availability of crystal structures has greatly improved our ability to build potent small molecule inhibitors. Intimate knowledge of the shape of the binding pocket greatly enhances the lead optimization process. For kinase targets in particular, a large body of information exists as to the variety of scaffolds that can be accommodated by the active site. This wealth of information has increased the speed at which we discover small molecules that bind with high affinity to kinase targets.

Accurately measuring the binding affinities of potential lead molecules is important for determining both isoform and kinase selectivity and may be important in selecting the best lead scaffold. For many of these kinases, the biological roles of the various isoforms that may exist is not always clear. Early characterization of scaffold selectivity can help in the early identification of selective scaffolds as the functions of the various isoforms continue to be uncovered.

Current methods available to measure binding affinity for small molecules such as isothermal titration calorimetry, surface plasmon resonance, and fluorescence spectroscopic techniques are limited in their ability to measure high-affinity slow binding small molecule inhibitors. One of the challenges facing the above-mentioned methods is the need to work at low concentrations. Low concentrations can be difficult to measure and deliver accurately. An advantage of the thermal denaturation method is the ability to work at concentrations well above the binding affinity. Another difficulty faced by traditional methods for measuring binding affinity is the need to reach equilibrium while at these low concentrations. This can be especially challenging when working with molecules such as the diaryl urea p38 MAPK inhibitors that have slow binding kinetics. Again the ability to work at concentrations where binding is not kinetically limited appears to alleviate this problem. The major disadvantage of the thermal denaturation method is the need for large quantities of protein relative to surface plasmon resonance and fluorescence methods.

The thermal denaturation method as presented in this paper is not optimized for the throughput required for drug discovery. In its current format, the method is medium throughput at best. The utility of this method lies in the fact that it does not require any specialized equipment. Melting temperatures can be easily generated using a UV−Vis spectrophotometer with an attached Peltier device. For a given protein target melting temperatures alone can be used to rank compounds with similar binding enthalpies. Converting these melting temperatures to binding affinities only requires measuring a few of the basic thermodynamic parameters for your system. Use of this technique for measuring the molecular potency as a tool to develop SAR for the diaryl urea class of p38α MAPK inhibitors is nicely shown in the following paper by Regan et al.[7] Until high throughput high sensitivity differential scanning calorimeters[15] or comparable technologies[16] are more widely available this is a viable method for acquiring this type

of information in a medium throughput mode of compound testing.

Acknowledgment. The authors would like to thank Alistair Baptiste, Gerry Bell, Elda Gautschi, and Teresa Molinaro for their assistance in performing experimental procedures. Useful discussions with Christine Grygon and Neil Moss are also gratefully acknowledged.

References

(1) Pargellis, C. A.; Tong, L.; Churchill, L.; Cirillo, P. F.; Gilmore, T.; Graham, A. G.; Grob, P. M.; Hickey, E. R.; Moss, N.; Pav, S.; Regan, J. Inhibition of p38 map kinase by utilizing a novel allosteric binding site. *Nat. Struct. Biol.* **2002**, *9*, 268−272.

(2) Brandts, J. F.; Lin, L. N. Study of Strong to Ultratight Protein Interactions Using Differential Scanning Calorimetry. *Biochemistry* **1990**, *29*, 6927−6940.

(3) Straume, M.; Freire, E. Two-Dimensional Scanning Calorimetry: Simultaneous Resolution of Intrinsic Protein Structural Energetics and Ligand Binding Interactions by Global Linkage Analysis. *Anal. Biochem.* **1992**, *203*, 259−268.

(4) Hinz, H.-J. Thermodynamic Parameters for Protein−Protein and Protein−Ligand Interaction by Differential Scanning Microcalorimetry. *Methods Enzymol.* **1986**, *130*, 59−79.

(5) Schwarz, F. P. Interaction of Cytidine 3′-Monophosphate and Uridine 3′-Monophosphate with Ribonuclease *a* at the Denaturation Temperature. *Biochemistry* **1988**, *27*, 8429−8436.

(6) Schellman, J. A. Macromolecular Binding. *Biopolymers* **1975**, *14*, 999−1018.

(7) Regan, J.; Capolino, A.; Cirillo, P. F.; Gilmore, T.; Graham, A. G.; Hickey, E.; Kroe, R. R.; Madwed, J.; Moriak, M.; Nelson, R.; Pargellis, C. A.; Swinamer, A.;Torcellini, C.; Tsang, M.; Moss, N. Structure−Activity Relationships of the p38 MAP Kinase Inhibitor BIRB 796. *J. Med. Chem.* **2003**, *46*, 4676−4686.

(8) Tong, L.; Pav, S.; White, D. M.; Rogers, S.; Crane, K. M.; Cywin, C. L.; Brown, M. L.; Pargellis, C. A. A highly specific inhibitor of human p38 Map kinase binds in the ATP pocket. *Nat. Struct. Biol.* **1997**, *4* (4), 311−316.

(9) Bevington, P. R. *Data Reduction and Error Analysis for the Physical Sciences*; McGraw-Hill: New York, 1969.

(10) Taylor, J. R. *An Introduction to Error Analysis*, 2nd ed.; University Science Books, Sausalito, CA, 1997.

(11) Fuller, W. A. *Measurement Error Models*; Jossey-Bass: New York, 1987.

(12) Roy, T. Fitting a Straight Line When Both Variables are Subject to Error: Pharmaceutical Applications. *J. Pharm. Biomed. Anal.* **1994**, *12*, 1265−1269.

(13) Regan, J.; Breitfelder, S.; Cirillo, P.; Gilmore, T.; Graham, A. G.; Hickey, E.; Klaus, B.; Madwed, J.; Moriak, M.; Moss, N.; Pargellis, C.; Pav, S.; Proto, A.; Swinamer, A.; Tong, L.; Torcellini, C. Pyrazole Urea-Based Inhibitors of p38 Map Kinase: From Lead Compound to Clinical Candidate. *J. Med. Chem.* **2002**, *45*, 2994−3008.

(14) Dumas, J. Protein kinase inhibitors: emerging pharmacophores 1997−2000. *Exp. Opin. Ther. Pat.* **2001**, *11*, 405−429.

(15) Plotnikov, V.; Rochalski, A.; Brandts, M.; Brandts, J. F.; Williston, S.; Frasca, V.; Lin, L. N. An Autosampling Differential Scanning Calorimeter Instrument for Studying Molecular Interactions. *ASSAY Drug Dev. Techn.* **2002**, *1* (1), 83−90.

(16) Pantoliano, M. W.; Petrella, E. C.; Kwansoski, J. D.; Lovanov, V. S.; Myslik, J.; Graf, E.; Carver, T.; Asel, E.; Springer, B. A.; Lane, P.; Salemme, F. R. High-Density Miniaturized Thermal Shift Assays as a General Strategy for Drug Discovery. *J. Biomol. Screening* **2001**, *6*, 429−440.

JM030120S